

## Dimensionality-Controlled Insulator-Metal Transition and Correlated Metallic State in 5d Transition Metal Oxides $\text{Sr}_{n+1}\text{Ir}_n\text{O}_{3n+1}$ ( $n = 1, 2, \text{ and } \infty$ )

S. J. Moon,<sup>1</sup> H. Jin,<sup>2</sup> K. W. Kim,<sup>3</sup> W. S. Choi,<sup>1</sup> Y. S. Lee,<sup>4</sup> J. Yu,<sup>2</sup> G. Cao,<sup>5</sup> A. Sumi,<sup>6</sup>  
H. Funakubo,<sup>6</sup> C. Bernhard,<sup>3</sup> and T. W. Noh<sup>1,\*</sup>

<sup>1</sup>ReCOE & FPRD, Department of Physics and Astronomy, Seoul National University, Seoul 151-747, Korea

<sup>2</sup>CSCMR & FPRD, Department of Physics and Astronomy, Seoul National University, Seoul 151-747, Korea

<sup>3</sup>Department of Physics and Fribourg Center for Nanomaterials, University of Fribourg, CH-1700 Fribourg, Switzerland

<sup>4</sup>Department of Physics, Soongsil University, Seoul 156-743, Korea

<sup>5</sup>Department of Physics and Astronomy, University of Kentucky, Lexington, Kentucky 40506, USA

<sup>6</sup>Department of Innovative and Engineered Materials, Interdisciplinary Graduate School of Science and Engineering, Tokyo Institute of Technology, Yokohama 226-8502, Japan

(Received 14 July 2008; published 24 November 2008)

We investigated the electronic structures of the 5d Ruddlesden-Popper series  $\text{Sr}_{n+1}\text{Ir}_n\text{O}_{3n+1}$  ( $n = 1, 2, \text{ and } \infty$ ) using optical spectroscopy and first-principles calculations. As 5d orbitals are spatially more extended than 3d or 4d orbitals, it has been widely accepted that correlation effects are minimal in 5d compounds. However, we observed a Mott insulator-metal transition with a change of bandwidth as we increased  $n$ . In addition, the artificially synthesized perovskite  $\text{SrIrO}_3$  showed a very large mass enhancement of about 6, indicating that it was in a correlated metallic state.

DOI: 10.1103/PhysRevLett.101.226402

PACS numbers: 71.30.+h, 71.20.-b, 78.20.-e

Mott physics, driven by electron correlation, has been an essential foundation for understanding the emergent properties of strongly correlated electron systems, including 3d and 4d transition metal oxides (TMOs) [1]. According to the Hubbard model, such systems can be characterized by the on-site Coulomb interaction  $U$  and the bandwidth  $W$ . When  $W \ll U$ , the system is in an insulating state, the so-called Mott insulator. When  $W \geq U$ , an insulator-metal transition (IMT) occurs and the system becomes metallic. Close to the IMT, the conducting carriers have a large effective mass due to electron correlation. This correlated metallic state (CMS) has unique physical properties, which cannot be explained by simple band theory. Therefore, the  $W$ -controlled IMT and associated CMS, especially in 3d and 4d TMOs, have been important subjects in condensed matter physics [1–4].

The 5d orbitals are spatially more extended than the 3d and 4d orbitals, so their  $W$  ( $U$ ) values should be larger (smaller) than 3d and 4d orbitals. In addition, the electron correlation should play a much smaller role. Therefore, many 5d TMOs have metallic ground states that can be described by the band theory [5,6]. However, some 5d TMOs, such as  $\text{Sr}_2\text{IrO}_4$ ,  $\text{Sr}_3\text{Ir}_2\text{O}_7$ , and  $\text{Ba}_2\text{NaOsO}_6$ , have insulating ground states [7–9]. There have been some recent reports that correlation effects could be important for the 5d insulating TMO [9,10]. This raises a couple of important questions. First, is it possible that an IMT occurs in 5d TMOs by systematically varying  $W$ ? Second, can the associated CMS be found in such a 5d TMO system?

Recently, we found that the unusual insulating state of  $\text{Sr}_2\text{IrO}_4$  could be explained by cooperative interaction between electron correlation and spin-orbit (SO) coupling [11]. The SO coupling constant of 5d TMOs is about 0.3–

0.4 eV [6], which is much larger than that of 3d TMOs ( $\sim 20$  meV) [12]. As the SO coupling constant of 5d TMOs is comparable to their  $U$  value of approximately 0.5 eV [11], it can cooperate with  $U$ . This cooperation should play an important role in their electronic structures [13]. The SO coupling can induce the formation of  $J_{\text{eff},1/2}$  and  $J_{\text{eff},3/2}$  bands, which are occupied by five electrons [14]. The  $J_{\text{eff},1/2}$  bands can be very narrow due to a decreased hopping integral caused by the isotropic orbital and mixed spin

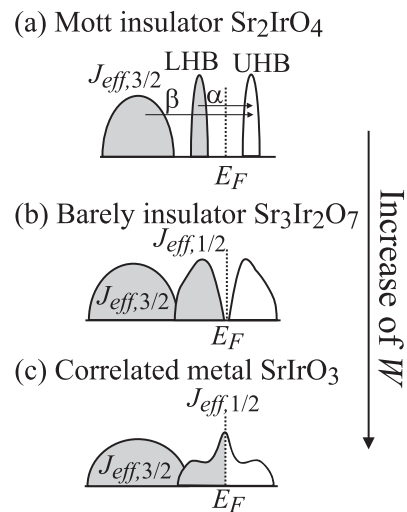


FIG. 1. Schematic band diagrams of 5d  $\text{Sr}_{n+1}\text{Ir}_n\text{O}_{3n+1}$  compounds, which are well described by the effective total angular momentum  $J_{\text{eff}}$  states due to strong spin-orbit coupling: (a) Mott insulator  $\text{Sr}_2\text{IrO}_4$ , (b) barely insulator  $\text{Sr}_3\text{Ir}_2\text{O}_7$ , and (c) correlated metal  $\text{SrIrO}_3$ .  $E_F$  represents the Fermi level and the arrow indicates the direction for the bandwidth  $W$  increase.

characters [11]. As shown schematically in Fig. 1(a), the effect of  $U$  can split the narrow  $J_{\text{eff},1/2}$  bands into a lower Hubbard band (LHB) and an upper Hubbard band (UHB), opening a Mott gap.

The weakly correlated narrow band system is a good starting point from which to search for the IMT by varying  $W$  and the associated CMS in  $5d$  TMOs. There are four neighboring Ir atoms  $z$  in  $\text{Sr}_2\text{IrO}_4$ . As  $W$  should be proportional to  $z$ , we could increase  $W$  by increasing the  $z$  value. Among the Ruddlesden-Popper series  $\text{Sr}_{n+1}\text{Ir}_n\text{O}_{3n+1}$  compounds, the  $z$  values for  $\text{Sr}_3\text{Ir}_2\text{O}_7$  and perovskite  $\text{SrIrO}_3$  are 5 and 6, respectively. In nature, however, bulk  $\text{SrIrO}_3$  has a hexagonal crystal structure at room temperature and atmospheric pressure. It transforms to the perovskite structure only at a higher pressure and temperature [15]. Therefore it was essential to obtain a perovskite  $\text{SrIrO}_3$  for the investigation.

In this Letter, we investigated the electronic structures of Ruddlesden-Popper series  $\text{Sr}_{n+1}\text{Ir}_n\text{O}_{3n+1}$  ( $n = 1, 2,$  and  $\infty$ ) compounds using optical spectroscopy and first-principles calculations. We artificially fabricated the perovskite  $\text{SrIrO}_3$  phase by growing an epitaxial thin film on a  $\text{MgO}$  substrate. We found that the  $W$  of Ir  $5d$  bands increased with the dimensionality or the  $z$  value. As shown schematically in Figs. 1(b) and 1(c), the IMT occurred between  $\text{Sr}_3\text{Ir}_2\text{O}_7$  and  $\text{SrIrO}_3$ . From the optical conductivity spectrum  $\sigma(\omega)$ , we also found that conducting carriers in the artificially fabricated  $\text{SrIrO}_3$  should have a large mass enhancement, indicating a CMS.

Single crystals of  $\text{Sr}_2\text{IrO}_4$  and  $\text{Sr}_3\text{Ir}_2\text{O}_7$  were grown using the flux technique [7,8]. To obtain a perovskite  $\text{SrIrO}_3$  sample, we grew epitaxial  $\text{SrIrO}_3$  thin film on cubic  $\text{MgO}$  (001) substrate. The cubic symmetry of the  $\text{MgO}$  substrate ensured that the  $\text{SrIrO}_3$  film grew in the perovskite phase [16]. The insets of Fig. 2(c) show the x-ray diffraction pattern and pole figure of the  $\text{SrIrO}_3$  film. The x-ray diffraction pattern showed that the  $\text{SrIrO}_3$  film was grown epitaxially in the perovskite form without any impurity phase. The x-ray pole figure measured around the (011) reflection of the  $\text{SrIrO}_3$  film showed that it had the fourfold symmetry of a (001) oriented perovskite structure. The epitaxial stabilization of the perovskite  $\text{SrIrO}_3$  phase enabled us to investigate the electronic structure changes of the iridates with  $W$  systematically.

We measured  $ab$  plane reflectance spectra of  $\text{Sr}_2\text{IrO}_4$  and  $\text{Sr}_3\text{Ir}_2\text{O}_7$  single crystals at room temperature. The corresponding  $\sigma(\omega)$  were obtained using the Kramers-Kronig transformation. For the  $\text{SrIrO}_3$  thin films, we measured reflectance and transmittance spectra in the energy region between 0.15 and 6 eV. By solving the Fresnel equations numerically [17], we obtained  $\sigma(\omega)$  for  $\text{SrIrO}_3$ . Between 0.01 and 0.09 eV, we used the far-infrared ellipsometry technique to obtain  $\sigma(\omega)$  directly [18]. Because of the strong phonon absorption of the  $\text{MgO}$  substrate, we could not obtain  $\sigma(\omega)$  between 0.09 and 0.15 eV.

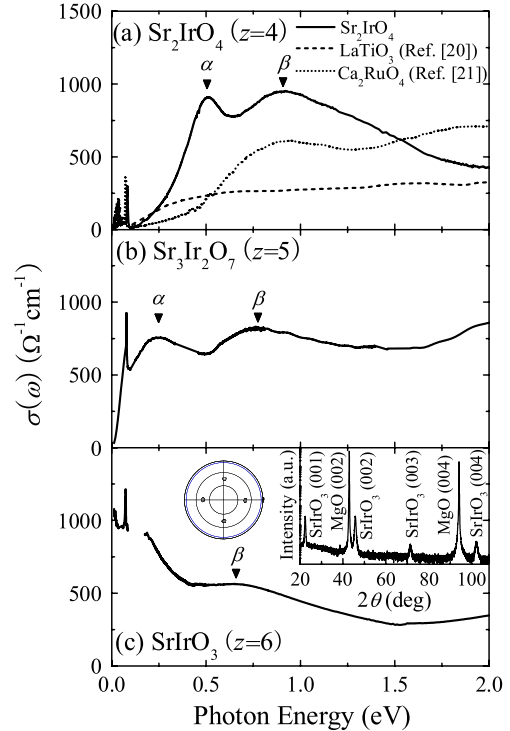


FIG. 2 (color online). Optical conductivity spectra  $\sigma(\omega)$  of (a)  $\text{Sr}_2\text{IrO}_4$ , (b)  $\text{Sr}_3\text{Ir}_2\text{O}_7$ , and (c)  $\text{SrIrO}_3$ . In (a),  $\sigma(\omega)$  of other Mott insulators, such as  $3d$   $\text{LaTiO}_3$  (Ref. [20]) and  $4d$   $\text{Ca}_2\text{RuO}_4$  (Ref. [21]), are shown for comparison. Peak  $\alpha$  corresponds to the optical transition from the LHB to the UHB of the  $J_{\text{eff},1/2}$  states. Peak  $\beta$  corresponds to the transition from the  $J_{\text{eff},3/2}$  bands to the UHB. The insets of (c) show the x-ray pole figure (left) and diffraction pattern (right) of the perovskite  $\text{SrIrO}_3$  film. The pole figure was measured around the (011) reflection of the  $\text{SrIrO}_3$  film.

Figure 2 shows that the  $\text{Sr}_{n+1}\text{Ir}_n\text{O}_{3n+1}$  compounds experienced IMT when the  $z$  value, i.e., the  $W$  value, was increased. For the  $z = 4$  compound  $\text{Sr}_2\text{IrO}_4$ ,  $\sigma(\omega)$  showed a finite-sized optical gap. For the  $z = 5$  compound  $\text{Sr}_3\text{Ir}_2\text{O}_7$ , the optical gap became almost zero. For the  $z = 6$  compound  $\text{SrIrO}_3$ , the optical gap finally disappeared, and a Drude-like response from conducting carriers appeared in the low frequency region. These spectral changes indicate that an IMT occurs between  $\text{Sr}_3\text{Ir}_2\text{O}_7$  and  $\text{SrIrO}_3$ .

It should be noted that  $\sigma(\omega)$  of  $\text{Sr}_2\text{IrO}_4$  has unique spectral features [19] that are difficult to find in most other Mott insulators. It has a double peak structure, marked as  $\alpha$  and  $\beta$  in Fig. 2(a). As shown in Fig. 1(a), peak  $\alpha$  can be assigned as an optical transition from the LHB to the UHB of the  $J_{\text{eff},1/2}$  states, while peak  $\beta$  can be assigned as that from the  $J_{\text{eff},3/2}$  bands to the UHB. Note that peak  $\alpha$  is very narrow with a width 3–5 times smaller than those of the correlation-induced peaks in other  $3d$  and  $4d$  Mott insulators. For comparison, in Fig. 2(a), we plotted the reported  $\sigma(\omega)$  of  $\text{LaTiO}_3$  and  $\text{Ca}_2\text{RuO}_4$  [20,21], which are well-known Mott insulators. The sharpness of peak  $\alpha$  originated from the narrowness of the SO coupling-triggered  $J_{\text{eff},1/2}$

Hubbard bands, which could facilitate the IMT driven by the increase of  $W$  with a small  $U$  value of a  $5d$  TMO.

To gain insight into the electronic structure changes of  $\text{Sr}_{n+1}\text{Ir}_n\text{O}_{3n+1}$ , we performed local density approximation (LDA) +  $U$  calculations with SO coupling included [22]. We used a  $U$  value of 2.0 eV, which produced electronic structures consistent with our experimental  $\sigma(\omega)$ . Most band structure calculations on  $3d$  Mott insulators have usually taken a  $U$  value of 4–7 eV [12]. Figures 3(a)–3(c) show the band dispersions of  $\text{Sr}_2\text{IrO}_4$ ,  $\text{Sr}_3\text{Ir}_2\text{O}_7$ , and  $\text{SrIrO}_3$ , respectively. In the energy region between  $-2.5$  and  $0.5$  eV, the Ir  $5d$   $t_{2g}$  states were the main contributors. The light and dark lines represent the  $J_{\text{eff},1/2}$  and  $J_{\text{eff},3/2}$  bands, respectively. For  $\text{Sr}_3\text{Ir}_2\text{O}_7$  and  $\text{SrIrO}_3$ , the  $J_{\text{eff},1/2}$  bands split due to the increase in interlayer coupling. When  $z$  increased, the neighboring Ir ions along the  $c$  axis had stronger hybridization of the  $d$  bands through the apical O ions. The hybridization split the bands into bonding and antibonding states, which resulted in an increase in  $W$ .

Figures 3(d)–3(f) show the total density of states (DOS) of  $\text{Sr}_2\text{IrO}_4$ ,  $\text{Sr}_3\text{Ir}_2\text{O}_7$ , and  $\text{SrIrO}_3$ , respectively. The  $J_{\text{eff},3/2}$  states contributed strongly to the DOS between  $-0.5$  and  $-1.5$  eV. In Figs. 3(d) and 3(e), the DOS between 0 and  $0.5$  eV ( $-0.5$  eV) was from the UHB (LHB) of the  $J_{\text{eff},1/2}$  states. In Fig. 3(f), the DOS between  $-0.5$  and  $0.5$  eV was from the  $J_{\text{eff},1/2}$  bands. For  $\text{Sr}_2\text{IrO}_4$ , the separation between the centers of the UHB and LHB ( $J_{\text{eff},3/2}$  bands) was approximately 0.5 eV (1.0 eV), consistent with the position of peak  $\alpha$  ( $\beta$ ) in Fig. 2(a). As  $z$  increased, the  $J_{\text{eff},1/2}$  and  $J_{\text{eff},3/2}$  bands clearly broadened. The  $W$  values of the

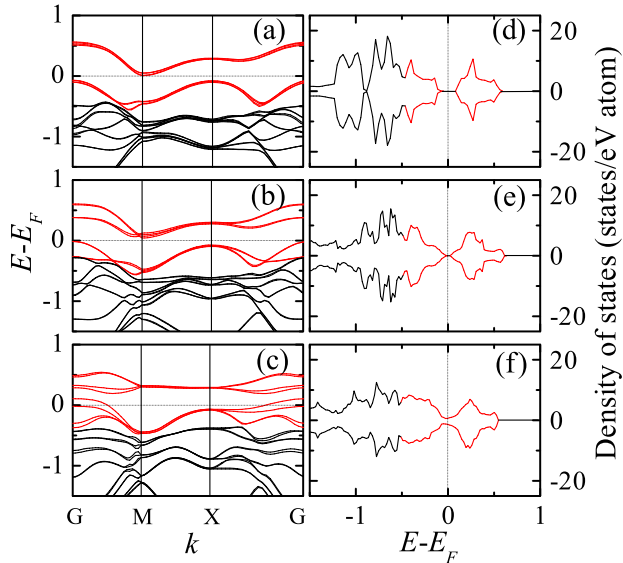


FIG. 3 (color online). Results from the LDA +  $U$  calculations including spin-orbit coupling: Band structures of (a)  $\text{Sr}_2\text{IrO}_4$ , (b)  $\text{Sr}_3\text{Ir}_2\text{O}_7$ , and (c)  $\text{SrIrO}_3$ , and total DOS of (d)  $\text{Sr}_2\text{IrO}_4$ , (e)  $\text{Sr}_3\text{Ir}_2\text{O}_7$ , and (f)  $\text{SrIrO}_3$ . The positive and negative DOS values represent spin-up and spin-down bands, respectively. The light and dark lines represent the  $J_{\text{eff},1/2}$  and  $J_{\text{eff},3/2}$  bands, respectively.

$J_{\text{eff},1/2}$  bands in the DOS were estimated to be about 0.48, 0.56, and 1.01 eV. As the  $J_{\text{eff},1/2}$  bands broadened, the Mott gap closed. These first-principles calculations demonstrate that an increase in  $W$  due to the dimensionality increase induces the IMT in  $\text{Sr}_{n+1}\text{Ir}_n\text{O}_{3n+1}$ .

Experimental evidence for the systematic changes in  $W$  of the  $J_{\text{eff},1/2}$  bands was obtained from  $\sigma(\omega)$ . As shown in Fig. 2, peaks  $\alpha$  and  $\beta$  broadened and decreased in energy with the increase of  $z$ . For quantitative analysis, we fitted  $\sigma(\omega)$  using the Lorentz oscillator model. For the insulators, we used three Lorentz oscillators, which corresponded to peaks  $\alpha$ ,  $\beta$ , and a charge transfer excitation from the O  $2p$  bands to the Ir  $5d$  bands. For  $\text{SrIrO}_3$ , we used the Drude model for metallic response and two Lorentz oscillators which corresponded to peak  $\beta$  and the charge transfer excitation. From this analysis, we obtained the peak positions and widths of peaks  $\alpha$  and  $\beta$ , i.e.,  $\omega_\alpha$ ,  $\omega_\beta$ ,  $\gamma_\alpha$ , and  $\gamma_\beta$ . According to Fermi's golden rule,  $\sigma(\omega)$  should be proportional to a matrix element and a joint density of states. Therefore, the width of an absorption peak should reflect the  $W$  of the initial and final bands. As shown in Fig. 4(a), both the  $\gamma_\alpha$  and  $\gamma_\beta$  values increased as  $z$  became larger. This confirmed that the IMT in  $\text{Sr}_{n+1}\text{Ir}_n\text{O}_{3n+1}$  should be driven by the change in  $W$ .

The Lorentz oscillator model analysis provided further information on the electronic structure changes. As shown in Fig. 4(a), both the  $\omega_\alpha$  and  $\omega_\beta$  values decreased system-

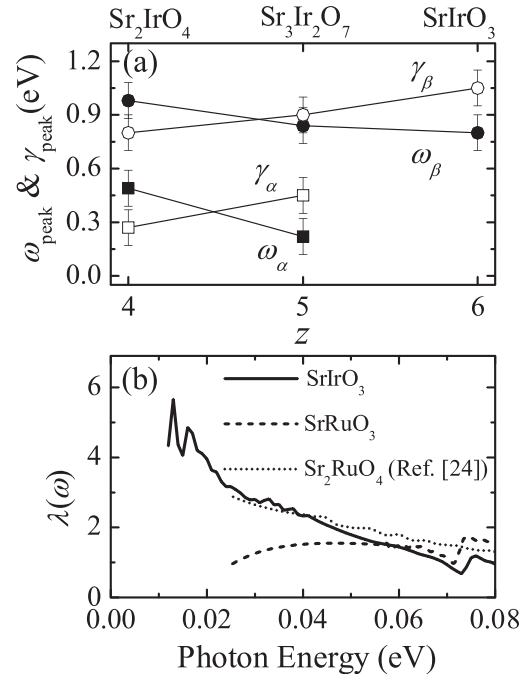


FIG. 4. (a) Results from Lorentz oscillator model analysis. The solid symbols show the positions of the  $\alpha$  and  $\beta$  peaks, i.e.,  $\omega_\alpha$  and  $\omega_\beta$ . The open symbols indicate the widths of the  $\alpha$  and  $\beta$  peaks, i.e.,  $\gamma_\alpha$  and  $\gamma_\beta$ . (b) Frequency-dependent mass enhancement  $\lambda(\omega)$  of correlated metal  $\text{SrIrO}_3$ . The  $\lambda(\omega)$  data of  $\text{SrRuO}_3$  (our data) and  $\text{Sr}_2\text{RuO}_3$  (Ref. [24]) are included for comparison.

atically as  $z$  was increased. The peak shift might originate from the increase of the spectral weight in the gap region, which would fill the Mott gap with increasing  $W$  [4]. For the  $\omega_\alpha$  change, the electronic structure changes for both LHB and UHB are important. However, the  $\omega_\beta$  change only involves changes in the UHB. In Fig. 4(a), the change in  $\omega_\alpha$  between  $\text{Sr}_2\text{IrO}_4$  and  $\text{Sr}_3\text{Ir}_2\text{O}_7$  was approximately  $0.25 \pm 0.05$  eV. Conversely, the change in  $\omega_\beta$  was approximately  $0.13 \pm 0.05$  eV, which is about half of the change in  $\omega_\alpha$ . This suggested that the electronic structure changes should occur symmetrically around the Fermi level for both Hubbard bands, as shown in Fig. 1.

To obtain firm evidence for Mott instability in  $5d$   $\text{Sr}_{n+1}\text{Ir}_n\text{O}_{3n+1}$ , we performed extended Drude model analysis on metallic  $\text{SrIrO}_3$  [23,24]. From the optical spectra, we obtained the mass enhancement of conducting carriers  $\lambda(\omega)$ , which corresponded to the effective mass normalized by the band mass. Substantial enhancement of  $\lambda(\omega)$  near the IMT is a hallmark of Mott instability and the corresponding compound should be in CMS. As shown in Fig. 4(b), the  $\lambda(\omega)$  of  $\text{SrIrO}_3$  reached about 6 at the lowest energy. We are not aware of any report on  $\lambda(\omega)$  for  $5d$  TMOs, so we included the room temperature  $\lambda(\omega)$  of  $4d$  correlated metals  $\text{SrRuO}_3$  and  $\text{Sr}_2\text{RuO}_4$  in Fig. 4(b) for comparison. The  $\lambda(\omega)$  of  $3d$  correlated metal (Ca, Sr) $\text{VO}_3$  was reported to be approximately 3–4 [25]. Note that the  $\lambda(\omega)$  of  $\text{SrIrO}_3$  is comparable to or larger than those of the  $3d$  and  $4d$  TMOs. It is interesting that such a large value of  $\lambda(\omega)$  was found for the  $5d$  TMO compound. This large value implies that  $\text{SrIrO}_3$  is a correlated metal close to the Mott transition.

Our unique findings, the IMT with respect to change in  $W$  and the large effective mass of the resulting metallic compound in  $5d$  system, challenge the conventional expectation that electron correlation is insignificant in  $5d$  systems. These results originated from the large SO coupling of  $5d$  transition metal ions. Recent theoretical results showed that the SO coupling in a  $4d$  counterpart compound could modify the Fermi surface within the metallic phase [26,27]. However, the large SO coupling in  $5d$  systems could drastically enhance the effect of the electron correlation. This cooperative interaction drives some  $5d$  TMOs close to the Mott instability.

In summary, we investigated the electronic structures of a weakly correlated narrow band system,  $5d$   $\text{Sr}_{n+1}\text{Ir}_n\text{O}_{3n+1}$ , using optical spectroscopy and first-principles calculations. We observed an insulator-metal transition driven by the bandwidth change and the associated correlated metallic state with a large effective mass. Our results clearly demonstrate that electron correlation could play an important role even in  $5d$  systems.

This work was financially supported by the Creative Research Initiative Program (Functionally Integrated

Oxide Heterostructure) of MOST/KOSEF, KOSEF through the ARP (R17-2008-033-01000-0), and Schweizer Nationalfonds with Grant No. 200020-119784. Y. S. L. was supported by the Soongsil University Research Fund. The experiments at PLS were supported in part by MOST and POSTECH.

\*twnoh@snu.ac.kr

- [1] M. Imada, A. Fujimori, and Y. Tokura, *Rev. Mod. Phys.* **70**, 1039 (1998).
- [2] A. Fujimori *et al.*, *Phys. Rev. Lett.* **69**, 1796 (1992).
- [3] J. S. Lee *et al.*, *Phys. Rev. B* **64**, 245107 (2001).
- [4] I. Kézsmárki *et al.*, *Phys. Rev. Lett.* **93**, 266401 (2004).
- [5] L. F. Mattheiss, *Phys. Rev.* **181**, 987 (1969).
- [6] L. F. Mattheiss, *Phys. Rev. B* **13**, 2433 (1976).
- [7] G. Cao *et al.*, *Phys. Rev. B* **57**, R11039 (1998).
- [8] G. Cao *et al.*, *Phys. Rev. B* **66**, 214412 (2002).
- [9] A. S. Erickson *et al.*, *Phys. Rev. Lett.* **99**, 016404 (2007).
- [10] H. J. Xiang and M.-H. Whangbo, *Phys. Rev. B* **75**, 052407 (2007).
- [11] B. J. Kim *et al.*, *Phys. Rev. Lett.* **101**, 076402 (2008).
- [12] T. Mizokawa and A. Fujimori, *Phys. Rev. B* **54**, 5368 (1996).
- [13] K. Rossnagel and N. V. Smith, *Phys. Rev. B* **73**, 073106 (2006).
- [14] As we mapped  $t_{2g}$  orbital states ( $L = 2$ ) into  $L_{\text{eff}} = 1$ , the  $J_{\text{eff},1/2}$  states are higher in energy than the  $J_{\text{eff},3/2}$  states. See J. B. Goodenough, *Phys. Rev.* **171**, 466 (1968).
- [15] J. M. Longo, J. A. Kafalas, and R. J. Arnott, *J. Solid State Chem.* **3**, 174 (1971).
- [16] Y. K. Kim *et al.*, *Jpn. J. Appl. Phys.* **45**, L36 (2005); A. Sumi *et al.*, *Thin Solid Films* **486**, 182 (2005).
- [17] T. W. Noh *et al.*, *Phys. Rev. B* **46**, 4212 (1992).
- [18] C. Bernhard, J. Humlicek, and B. Keimer, *Thin Solid Films* **455–456**, 143 (2004).
- [19] S. J. Moon *et al.*, *Phys. Rev. B* **74**, 113104 (2006).
- [20] T. Arima, Y. Tokura, and J. B. Torrance, *Phys. Rev. B* **48**, 17006 (1993).
- [21] J. S. Lee *et al.*, *Phys. Rev. Lett.* **89**, 257402 (2002).
- [22] The LDA +  $U$  calculation may not be appropriate for a metallic system, as it cannot explicitly define the Hubbard bands of correlated metal. However, for the systematic comparison of the  $W$  change in  $\text{Sr}_{n+1}\text{Ir}_n\text{O}_{3n+1}$ , we presented the results of the LDA +  $U$  calculation with SO coupling for  $\text{SrIrO}_3$ . Since the structural information on the perovskite  $\text{SrIrO}_3$  phase was not available, we used the structural information of  $\text{SrRhO}_3$  in the calculations.
- [23] D. N. Basov and T. Timusk, *Rev. Mod. Phys.* **77**, 721 (2005).
- [24] J. S. Lee *et al.*, *Phys. Rev. Lett.* **96**, 057401 (2006).
- [25] H. Makino *et al.*, *Phys. Rev. B* **58**, 4384 (1998).
- [26] M. W. Haverkort *et al.*, *Phys. Rev. Lett.* **101**, 026406 (2008).
- [27] Guo-Qiang Liu *et al.*, *Phys. Rev. Lett.* **101**, 026408 (2008).